Journal of Hazardous Materials 211–212 (2012) 436–442

Contents lists available at SciVerse ScienceDirect

Journal of Hazardous Materials

journal homepage: www.elsevier.com/locate/jhazmat

Ecotoxicity of TiO_2 to *Daphnia similis* under irradiation

Glauciene P.S. Marcone [a], Ádria C. Oliveira [b], Gilberto Almeida [b], Gisela A. Umbuzeiro [b], Wilson F. Jardim [a,*]

[a] *Institute of Chemistry, UNICAMP, PO Box 6154, 13083-970, Campinas, SP, Brazil*
[b] *Faculty of Technology, State University of Campinas, UNICAMP, Limeira, SP, Brazil*

ARTICLE INFO

Article history:
Received 5 July 2011
Received in revised form
19 December 2011
Accepted 24 December 2011
Available online 9 January 2012

Keywords:
TiO_2
Nanoparticles
Daphnia similis
UV A and visible radiation
Ecotoxicity

ABSTRACT

Currently, there are a large number of products (sunscreen, pigments, cosmetics, plastics, toothpastes and photocatalysts) that use TiO_2 nanoparticles. Due to this large production, these nanoparticles can be released into the aquatic, terrestrial and aerial environments at relative high concentration. TiO_2 in natural water has the capacity to harm aquatic organisms such as the *Daphnia* (Cladocera) species, mainly because the photocatalytic properties of this semiconductor. However, very few toxicity tests of TiO_2 nanoparticles have been conducted under irradiation. The aim of this study was to evaluate anatase and rutile TiO_2 toxicity to *Daphnia similis* exploring their photocatalytic properties by incorporating UV A and visible radiation as a parameter in the assays. Anatase and rutile TiO_2 samples at the highest concentration tested (100 mg L^{-1}) were not toxic to *D. similis*, neither in the dark nor under visible light conditions. The anatase form and a mixture of anatase and rutile, when illuminated by a UV A black light with a peak emission wavelength of 360 nm, presented photo-dependent EC50 values of 56.9–7.8 mg L^{-1}, which indicates a toxicity mechanism caused by ROS (reactive oxygen species) generation.

1. Introduction

Nanoparticles are particles with one or more dimensions in the nanoscale range of 1–100 nm [1]. Several nanomaterials, such as nanosilver, fullerene (C60), carbon nanotubes and titanium dioxide are now constituents of many industrialized products from the pharmaceutical, automobile, textile, electronic, and cosmetic industries [2]. According to the Project on Emerging Nanotechnologies (PEN) [3] inventory, the number of products that use nanomaterials increased from 54 in 2005, to 1317 in 2010. From these, about 54 use TiO_2 in their composition. Examples are sunscreen, pigments, cosmetics and photocatalysts [4].

Due to the photocatalytic properties of TiO_2 when activated by UV radiation ($\lambda < 365$ nm), including sunlight, this material has been used in several environmental applications, exploring bactericidal effects as well as the destructive potential of numerous substances present in water and in air [5–8]. This same property that makes TiO_2 attractive to environmental applications can be dangerous to both the environment and human health [9–13].

Several studies have investigated the damage caused by TiO_2 to organisms in aquatic environments [14–16]. An overview of these studies with bacteria, Cladocera and algae species showed that TiO_2 is less harmful than other well known semiconductors in the nano range, such as ZnO and CuO [14].

TiO_2 photoactivation under UV radiation creates a redox pair, electron/hole (e^-/h^+) that in contact with adsorbed water on the TiO_2 surface causes ROS (reactive oxygen species) generation, mainly, $^{\bullet}OH$, H_2O_2 and $^1O_2$ [17–19]. These oxygen species can damage cell membranes and DNA leading to the inactivation of Gram negative and Gram positive bacteria and viruses [20–23].

The average concentration of TiO_2 used in a disinfection process mediated by UV radiation is in the range of 100–1000 mg L^{-1} [24], whereas ecotoxicological studies with aquatic organisms showed that toxic TiO_2 concentrations are much lower, around 1–100 mg L^{-1} [14].

Being a very active photocatalyst, it is expected that ecotoxicological evaluations involving TiO_2 must take into consideration photonic availability, especially in the spectral range in which the semiconductor can be excited. Furthermore, the way the photoactivity of TiO_2 has been explored so far in studies evaluating the toxicity of TiO_2 using *Daphnia* is questionable. Because the standard protocol indicates that test needs to be carried out in the dark or under a light/dark photoperiod, there have been some attempts use pre-illuminate TiO_2 before exposure of the test organism [25–27]. In this scenario, controversial results arose from the very few studies exploring photoactive TiO_2 characteristics when evaluating toxicity using *Daphnia*. Although Wiench et al. [25] showed

* Corresponding author. Tel.: +55 19 3521 3037.
E-mail addresses: gmarcone10@gmail.com (G.P.S. Marcone), wfjardim@iqm.unicamp.br (W.F. Jardim).

0304-3894/$ – see front matter © 2012 Elsevier B.V. All rights reserved.
doi:10.1016/j.jhazmat.2011.12.075

that a TiO_2 suspension UV–vis pre-illuminated for 30 minutes, did not increase TiO_2 toxicity, Hund-Rinke and Simon [26] observed an increase in the toxicity to *Daphnia magna* using this same approach.

Considering that photoactivation of TiO_2 compounds by UV–vis light can derive from both natural (sunlight shows a spectral distribution in the range of 200–700 nm) or artificial (black or white lamps) sources, two different radiation sources (UV A and visible light) were used in this paper. Considering this characteristics, the aim of this paper was to compare the acute toxicity of some TiO_2 nanoparticles results under both UV (emission range from 320 to 400 nm) and visible light (emission range from 400 to 800 nm), compared to dark conditions, following a standard protocol, using *D. similis*.

2. Materials and methods

2.1. Reagents

Aldrich titanium tetraisopropoxide and perchloric acid, 2-propanol (J.T. Baker), and tri-distilled water were used to synthesize different TiO_2 materials.

2.2. TiO_2 synthesis

Anatase and rutile TiO_2 were synthesized using the sol-gel method [28]. TiO_2 powder was heated at 400 °C and 900 °C, to obtain TiO_2 anatase (Anatase-S) and rutile (Rutile-S), respectively. A sample denominated M-S was obtained by mixing Anatase-S and Rutile-S in a 70:30 anatase/rutile ratio (w/w).

2.3. Commercial TiO_2

Commercial TiO_2, P25 Degussa (P25), containing 30% rutile and 70% anatase was also tested for toxicity, for comparison with the synthetic samples. P25 was calcined at 900 °C to obtain the sample denominated P 25* (commercial rutile).

2.4. Characterization of the nanomaterial

Crystalline phase, particle size, shape, agglomeration tendency and optical properties (energy band gap, E_g) of the TiO_2 were determined in the laboratory. The titanium dioxide powder was characterized by X ray diffraction (XRD), UV–vis diffuse reflectance spectroscopy (UV–vis DRS) and by Brunauer–Emmett–Teller (S_{BET}) surface area. 100 mg L^{-1} TiO_2 suspensions were prepared in distilled water and sonicated during 30 minutes in a Branson 2210 Ultrasonics equipment and then characterized by transmission electron microscopy (TEM) and UV–vis spectrophotometry. For toxicity testing, the TiO_2 suspensions were prepared with *Daphnia's* dilution water with added salts (KCl, $NaHCO_3$, $CaSO_4{\cdot}2H_2O$ and $MgSO_4{\cdot}7H_2O$) [29].

Crystalline phases were determined with a Shimadzu XDA diffractometer (Cu Kα, λ = 1.542 Å radiation). The size of the crystals was estimated using Scherrer's equation [30,31]. A Varian Cary 5G UV–vis–NIR spectrophotometer was used to obtain the diffuse reflectance spectra using $BaSO_4$ as background. Diffuse reflectance spectra were processed to obtain the F (R) equation in accordance with the Kubelka–Munk method [32–35]. Specific surface area was measured by the BET method using a Micrometrics Gemini 2375 instrument. The particle size and agglomeration degree were measured with a Zeiss Libra 120 high resolution field emission TEM. The UV–vis spectra were obtained with a Shimadzu UV-1601PC UV–vis spectrophotometer.

2.5. Testing organisms

Testing organisms were obtained from a culture of *D. similis*, a fresh water microcrustacea, cultivated in the Ecotoxicology and Environmental Microbiology Laboratory (LEAL) of the University of Campinas, in Limeira, SP, Brazil. Organisms were fed daily with algae (*Pseudokircheriella subcapitata*) and maintained at 20 ± 2 °C, under photoperiod (light/dark, 16:8) of illumination. The sensitivity of the *Daphnia* cultures was evaluated monthly using NaCl.

2.6. Toxicity testing

Concentrations from 1 to 100 mg L^{-1} TiO_2 of different TiO_2 samples (Anatase-S, Rutile-S, M-S, P25* and P25) were prepared in dilution water and sonicated during 30 min in a Branson 2210 ultrasonic bath before testing. Each concentration was tested in triplicate and blank controls were included (dilution water). Five neonates (under 24 h old) were added to each vial containing 10 mL of sample and incubated at 20 ± 2 °C under dark condition for 48 h following OECD [36] and ABNT Brazilian guidelines [37] that recommend of incubation conditions either under dark or using a visible light photoperiod (light/dark). Hardness, pH and conductivity were monitored before testing. Immobilized organisms were counted after 48 h. When the percentage of immobilized organisms in the control condition was less than 10%, the test was considered valid. EC50 (mg L^{-1}) was calculated using the Trimmed Sperman Karber (JSPEAR) software with a 95% confidence interval.

2.6.1. Exposure of Daphnia similis under UV A and visible radiation conditions: photoactivity of TiO_2

To explore the photoactive characteristics of TiO_2, three tests were performed simultaneously: (a) using the standard dark condition [36,37], (b) under UV A radiation, and (c) under visible radiation. The assays were performed in three boxes (50 cm × 50 cm × 35 cm) with lids (50 cm × 50 cm × 5 cm) built with medium-density-fiberboard (MDF). Constant temperature (20 ± 2 °C) was maintained by inserting a 8 cm diameter Microvent cooler. One lid had two 15 W UV fluorescent lamps (UVA) and the other lid a 15 W Xe fluorescent lamp (visible light). A third box without lamps was used to perform the test in the dark [36,37].

Table 1
Physicochemical parameters, crystallite size, Brunauer–Emmett–Teller surface area (S_{BET}), energy band gap (E_g), average particle size and average agglomerated size of the TiO_2 samples used in the toxicity tests.

Sample	% Crystalline form	Crystallite size (nm)	S_{BET} ($m^2\ g^{-1}$)	E_g (eV)	Average particle size[a] (nm)	Average agglomerated size[a] (nm)
P25	30% rutile; 70% anatase	19	49	3.37	25	400
M-S	30% rutile; 70% anatase	12	49	3.14	20	450
Anatase-S	100% anatase	10	57	3.02	19	330
Rutile-S	100% rutile	27	10	2.92	33	400
P25*	100% rutile	22	9	3.00	35	350

[a] These results were obtained from suspensions that were prepared using *Daphnia's* dilution water as solvent.

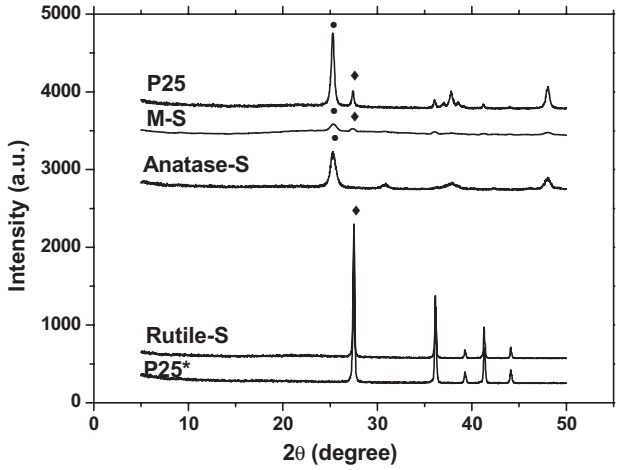

Fig. 1. X-ray diffractograms of TiO_2 samples, P25 (commercial sample containing 30% rutile and 70% anatase), M-S (synthesized sample containing 30% rutile and 70% anatase), Anatase-S (synthesized sample containing 100% anatase), Rutile-S (synthesized sample containing 100% rutile) and P25* (commercial sample containing 100% rutile). Symbols (●) Anatase and (♦) Rutile.

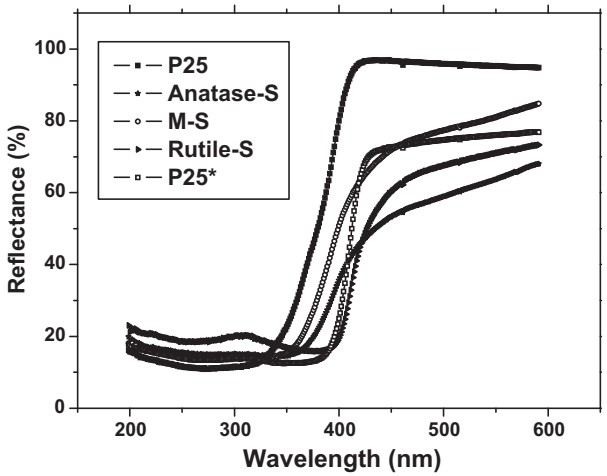

Fig. 2. UV–visible DRS spectra of TiO_2 samples: P25, M-S, Anatase-S, Rutile-S and P25*.

3. Results and discussion

3.1. Commercial and synthesized TiO_2 characterization

According to the X-ray diffractograms obtained, the predominant form of TiO_2 obtained were anatase and rutile (Fig. 1), as expected. Rutile-S and P25* samples showed only the rutile crystalline form, as can be observed the diffraction patterns, (1 1 0) at $2\theta = 27^\circ$, present in both diffractograms. Anatase is the only crystalline form present in the Anatase-S sample (diffraction peak (1 0 1) at $2\theta = 25^\circ$). As expected, a mixture of both forms (anatase and rutile) was found in the M-S and P25 samples.

The crystallite size of each sample was in the range of 10–27 nm and the surface area varied from 10 to 57 $m^2\ g^{-1}$ (Table 1). Samples containing predominantly anatase showed higher surface area than the rutile phase, probably due to the lower temperature synthesis of anatase [38,39].

Anatase-S, M-S and P25 samples presented band gap energy in the UV region of 390, 392 and 376 nm, respectively (Fig. 2). Rutile samples (Rutile-S and P25*) presented a band gap energy in the visible region around 405 nm. These values are in accordance with bulk TiO_2, but the blue shifted displacement is associated to the nanomaterial showing a size range of 5–10 nm [40,41].

Assuming direct optical transition, the function $[F(R)\ h\nu]^2$ was plotted against $h\nu = E_g$ (eV) (Fig. 3), and the results were obtained by extrapolation of $[F(R)\ h\nu]^2$ to zero [42]. E_g values for semiconductor

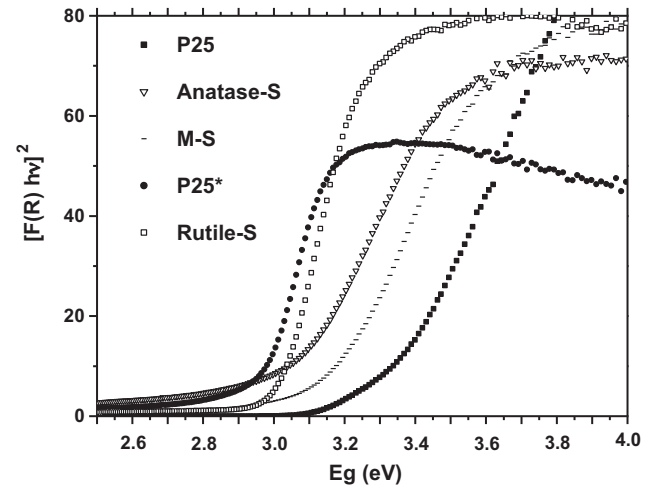

Fig. 3. The Kubelka–Munk transformed reflectance spectra for TiO_2 samples: P25, M-S, Anatase-S, Rutile-S and P25*.

photoactivation show that anatase samples showed higher band gap energy values than rutile samples (Fig. 3 and Table 1). Increased E_g values observed in the mixture of both phases (samples M-S and P25) could be explained by recombination rates e^-/h^+ [43–45].

The UV–vis spectra of TiO_2 suspensions have been used to characterize and quantify TiO_2 concentration using its maximum absorption at 329 nm [46]. An absorption band from 250 to 450 nm was observed with a maximum around 329 nm for P25 and

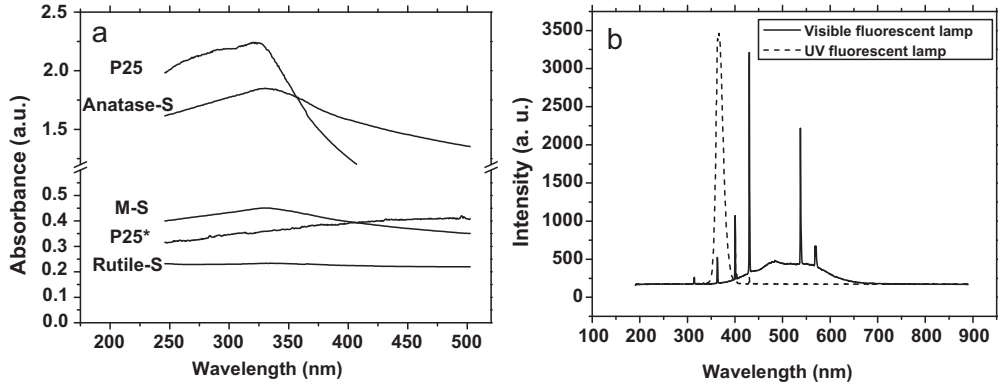

Fig. 4. (a) UV–visible spectra of TiO_2 samples: P25, M-S, Anatase-S, Rutile-S and P25*. (b) Emission spectra of the visible and UV A fluorescent lamps.

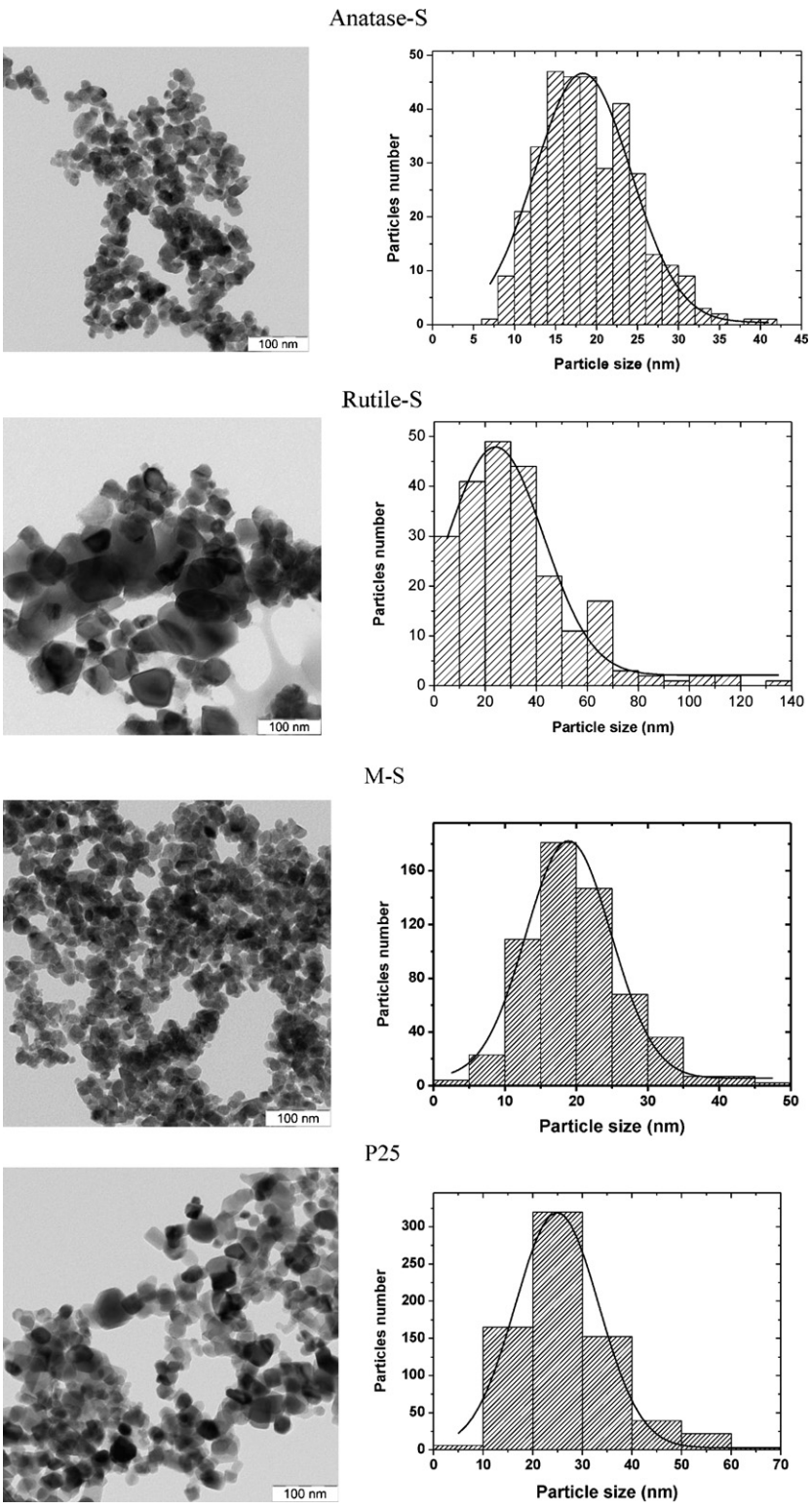

Fig. 5. TEM micrographs of TiO_2 samples presented as Anatase-S, Rutile-S, M-S and P25.

Anatase-S samples. M-S sample showed a discrete absorption band and P25* presented a greater tendency to absorption in the visible range ($\lambda > 400$ nm). Rutile-S, did not present a significant absorption (Fig. 4a).

According to the absorption wavelength regions observed for the tested samples, UVA and visible fluorescent lamps were used to promote the photoactivation of TiO_2. Emission spectra obtained for both lamps showed emission peaks at 365 nm for the UV A fluorescent lamp, from 450 to 600 nm for the visible fluorescent lamp (Fig. 4b).

To evaluate the ecotoxicity of nanomaterials, it is interesting to assess their physicochemical properties, especially size of TiO_2 particles and level of agglomeration in suspension. The TEM images show that the particle size of Anatase-S, M-S and P25 ranged from 19 to 25 nm (Fig. 5), and they tend to aggregate in larger particles in the 330–450 nm range (Table 1). Rutile-S sample showed particle

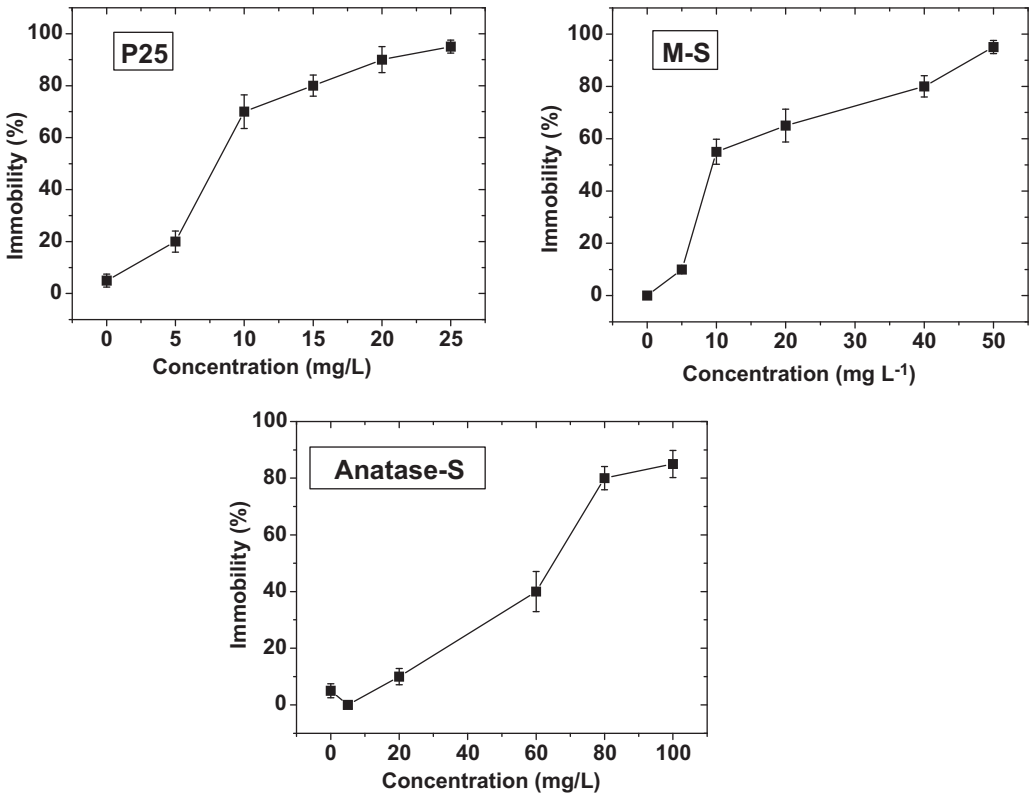

Fig. 6. Dose–response for P25, M-S and Anatase-S TiO_2 samples obtained in 48 h exposure tests using *D. similis*. Error bars are presented for each measurement ($n = 4$).

sizes of 35 nm and agglomerated in the same range as the other two particles.

3.2. Toxicity testing

Preliminary toxicity tests using *D. similis* were conducted with P25 and P25*, under the three light conditions already described (dark, UV A and visible radiation). Hardness values varied between 40 and 48 mg L^{-1} $CaCO_3$, pH 7.2–7.6 and conductivity around 160 μS cm^{-1}, which were in accordance with the method requirements.

P25 and P25* showed no toxicity in the dark at the maximum concentration (100 mg L^{-1}) tested (Table 2), in agreement with the literature. Warheit et al. [47] and Zhu et al. [48] observed an EC50 > 100 mg L^{-1} for TiO_2 (100–140 nm) for *D. magna* after 48 h of exposure. Wiench et al. [25] found EC50 > 100 mg L^{-1} for uncoated and coated nanoparticles and uncoated non-nano particles of TiO_2.

In general, smaller nanoparticles are more toxic to aquatic organisms than larger nanoparticles. This could be explained by the fact that smaller nanoparticles (<10 nm) penetrate into in the cells more easily [20,49]. Lovern and Klaper [50] reported that a sonicated TiO_2 suspension at a concentration of 50–500 mg L^{-1} did not show any toxicity to *D. magna* after 48 h exposure. However, the filtered solution (0.2 μm) showed an EC50 of 5.5 mg L^{-1}. Bang et al. [51] observed that P25 TiO_2 particles of 21 nm were not toxic to *D. magna* at a concentration of 40 mg L^{-1}, while nanoparticles of rutile TiO_2 of 500 nm and P25 TiO_2 of 250 nm nanoparticles were also not toxic to *D. magna* at a higher concentration (799 mg L^{-1}).

Acute toxicity tests using *Daphnia* species have been performed so far under questionable conditions when the objective was to explore the photoactivity of the TiO_2. Hund-Rinke et al. [26] observed that the toxicity of TiO_2 to *D. magna* increased using pre-illumination compared to the dark condition. Anatase TiO_2 suspensions (25 nm and 100 nm particles) in the range of 1–3 mg L^{-1} were pre-illuminated using a Xe fluorescent lamp (300–800 nm, 250 W) for 30 min. In this case, the pre-illumination time did not guarantee the production of reactive oxygen species as this generation is concomitant to the photons reaching the semiconductor [52]. Additionally, Marugán et al. [53] observed that •OH production is directly proportional to the TiO_2 photoactivation time, causing irreversible damage to *E. coli*.

In this work, when P25 and P25* were tested under visible radiation no toxicity was observed (EC50 > 100 mg L^{-1}) (Table 2). This can be explained by the low absorption of visible radiation by these materials in the spectral range (>400 nm) corresponding to the visible fluorescent lamp emission (Fig. 4).

Preliminary tests under UV A radiation showed that the nanomaterial denominated P25 was more toxic (EC50 < 20 mg L^{-1}) than P25* (EC50 > 100 mg L^{-1}) (Table 2). The data suggest that TiO_2 photoactivity under UV A radiation is the principal cause of the acute toxic effect of this nanomaterial. Tests with the anatase and rutile forms of TiO_2 (samples P25, M-S, Anatase-S and Rutile-S) were carried using multiple concentrations under UV A radiation for estimation of the EC50.

Table 2
Results expressed as EC50 (mg L^{-1}) values of the toxicity test using *D. similis* under UV A radiation for TiO_2 samples, P25, M-S, Anatase-S and Rutile-S. The table shows the preliminary results ([a]) of P25 and P25* under UV A and visible radiation and in the dark condition.

Samples	EC50 (mg L^{-1})		
	UV A radiation	Visible radiation	Dark
P25*	>100[a]	>100[a]	>100[a]
P25	7.8 (<20[a])	>100[a]	>100[a]
M-S	12.5	–	–
Anatase-S	56.9	–	–
Rutile-S	>100	–	–

TiO_2 samples used in tests with *D. similis* under different radiation conditions and in the dark condition (see Section 2 for more details).

[a] Preliminary results for P25 and P25* samples of TiO_2 in tests.

EC50 values and dose-responses curves for P25, M-S and Anatase-S are presented in Table 2 and Fig. 6, respectively. The toxicity order was P25 > M-S > Anatase-S > Rutile-S, which can be explained by the TiO_2 optical properties.

The crystalline form of anatase TiO_2 under UV A radiation presented a different toxic behavior when compared to rutile under the same conditions (Table 2). This behavior can be attributed to the photoactive property of the anatase and not only because of the aggregate sizes [54]. Rutile-S is constituted of aggregates of 400 nm (Fig. 5 and Table 1) and did not show any toxicity at 100 mg L^{-1}. This finding is also emphasized by three factors: photoactivation in the visible region (~405 nm); band gap energy (2.92 eV) of the sample and, especially, low UV absorption (Fig. 4a) at λ = 363 nm.

Although P25, M-S and Anatase-S presented similar particle size distributions and agglomerate sizes (Fig. 5 and Table 1), P25 and M-S were more toxic to *D. similis* than Anatase-S. This can be explained by the high recombination rate e^-/h^+ of P25 and M-S associated with the band gap values, 3.37 and 3.14 eV, respectively. Although Anatase-S showed an elevated absorption in UV–vis region (Fig. 4a), the E_g value (3.02 eV) explains the reduction in toxicity associated to the photoactivity when compared to P25 and M-S samples.

Toxicity mechanisms of TiO_2 for aquatic organisms are not yet fully understood. However its toxicity has been attributed mainly to ROS generation [41,46–49,55].

4. Conclusions

It is possible to perform toxicity tests on *D. similis* under UV A irradiation conditions and this should be a requirement in standard protocols when TiO_2 semiconductors (or other photoactive materials) are tested. Anatase and rutile forms did not present acute toxicity to *D. similis* either in the dark or under visible radiation when tested up to 100 mg L^{-1}. Samples of TiO_2 in the anatase form (Anatase-S) and a mixture of anatase and rutile (P25 and M-S) showed a UV A radiation photo-dependent toxicity to *D. similis*. P25 and M-S were about five times more toxic than Anatase-S. The ecotoxicity of other photoactive nanomaterials could be performed using the method developed in this paper.

Acknowledgements

We acknowledge FAPESP and INCTAA for financial support and C.H. Collins (IQ-UNICAMP, Brazil) for English revision.

References

[1] M. Farré, K. Gajda-Schrantz, L. Kantiani, D. Barceló, Ecotoxicity and analysis of nanomaterials in the aquatic environment, Anal. Bioanal. Chem. 393 (2009) 81–95.
[2] B. Nowack, T.D. Bucheli, Occurrence, behavior and effects of nanoparticles in the environment, Environ. Pollut. 150 (2007) 5–22.
[3] The Project on Emerging Nanotechnologies PEN, The first publicly available on-line inventory of nanotechnology-based consumer products. http://www.nanotechproject.org/inventories/consumer/analysis_draft/, 2011 (accessed 29.05.11).
[4] R.J. Aitken, M.Q. Chaudhry, A.B.A. Boxall, M. Hull, Manufacture and use of nanomaterials: current status in the UK and global trends, Occup. Med. 56 (2006) 300–306.
[5] W.F. Jardim, S.G. Moraes, M.M.K. Takiyama, Photocatalytic degradation of aromatic chlorinated compounds using TiO_2: toxicity of intermediates, Water Res. 31 (1997) 1728–1732.
[6] J.B. Gálvez, S.M. Rodríguez, C.A.E. Gasca, E.R. Bandala, S. Gelover, T. Leal, Purificación de aguas por fotocatálisis heterogénea: Estado del arte, in: M.A. Blesa (Ed.), Eliminación de Contaminantes por Fotocatálisis Heterogénea, La Plata, 2001, pp. 51–76.
[7] U.I. Gaya, A.H. Abdullah, Heterogeneous photocatalytic degradation of organic contaminants over titanium dioxide: a review of fundamentals, progress and problems, J. Photochem. Photobiol. C 9 (2008) 1–12.
[8] L. Rizzo, S. Meric, D. Kassinos, M. Guida, F. Russo, V. Belgiorno, Degradation of diclofenac by TiO_2 photocatalysis: UV absorbance kinetics and process evaluation through a set of toxicity bioassays, Water Res. 43 (2009) 979–988.
[9] Q. Li, S. Mahendra, D.Y. Lyon, L. Brunet, M.V. Liga, D. Li, P.J.J. Alvarez, Antimicrobial nanomaterials for water disinfection and microbial control: potential applications and implications, Water Res. 42 (2008) 4591–4602.
[10] A. Nemmar, K. Melghit, B.H. Ali, The acute proinflammatory and prothrombotic effects of pulmonary exposure to rutile TiO_2 nanorods in rats, Exp. Biol. Med. 233 (2008) 610–619.
[11] J.L. Kang, C. Moon, H.S. Lee, W.H. Lee, E.M. Park, H.S. Kim, V. Castranova, Comparison of the biological activity between ultrafine and fine titanium dioxide particles in RAW 264.7 cells associated with oxidative stress, J. Toxicol. Environ. Health A 71 (2008) 478–485.
[12] V.H. Grassian, A. Adamcakova-Dodd, J.M. Pettibone, P.T. O'shaughnessy, P.S. Thorne, Inflammatory response of mice to manufactured titanium dioxide nanoparticles: comparison of size effects through different exposure routes, Nanotoxicology 1 (2007) 211–226.
[13] D.B. Warheit, T.R. Webb, K.L. Reed, Pulmonary toxicity screening studies in male rats with TiO_2 particulates substantially encapsulated with progenically deposited amorphous silica, Part. Fibre Toxicol. 3 (2006) 1–9.
[14] A. Kahru, H. Dubourguier, From ecotoxicology to nanoecotoxicology, Toxicology 269 (2010) 105–119.
[15] J.R. Peralta-Videa, L. Zhaoa, M.L. Lopez-Morenoc, Nanomaterials and the environment: a review for the biennium 2008–2010, J. Hazard. Mater. 186 (2011) 1–15.
[16] K. Aschberger, C. Micheletti, B. Sokull-Klüttgen, F.M. Christensen, Analysis of currently available data for characterising the risk of engineered nanomaterials to the environment and human health-lessons learned from four case studies, Environ. Int. 37 (2011) 1143–1156.
[17] A.G. Rincón, C. Pulgarin, Photocatalytical inactivation of *E. coli*: effect of (continuous-intermittent) light intensity and of (suspended-fixed) TiO_2 concentration, Appl. Catal. B 44 (2003) 263–284.
[18] C. Chen, P. Lei, H. Ji, W. Ma, J. Zhao, Photocatalysis by titanium dioxide and polyoxometalate/TiO_2 cocatalysts. Intermediates and mechanistic study, Environ. Sci. Technol. 38 (2004) 329–337.
[19] J. Nowotny, Titanium dioxide-based semiconductors for solar-driven environmentally friendly applications: impact of point defects on performance, Energy Environ. Sci. 1 (2008) 565–572.
[20] G. Jiang, Z. Shen, J. Niu, Y. Bao, J. Chen, T. He, Toxicological assessment of TiO_2 nanoparticles by recombinant *Escherichia coli* bacteria, J. Environ. Monit. 13 (2011) 42–48.
[21] M. Cho, H. Chung, W. Choi, J. Yoon, Linear correlation between inactivation of *E. coli* and OH radical concentration in TiO_2 photocatalytic disinfection, Water Res. 38 (2004) 1069–1077.
[22] L. Zan, W. Fa, T.P. Peng, Z.K. Gong, Photocatalysis effect of nanometer TiO_2 and TiO_2-coated ceramic plate on hepatitis B virus, J. Photochem. Photobiol. B: Biol. 86 (2007) 165–169.
[23] P. Hajkova, P. Spatenka, J. Horsky, I. Horska, A. Kolouch, Photocatalytic effect of TiO_2 films on viruses and bacteria, Plasma Process. Polym. 4 (2007) S397–S401.
[24] C. Wei, W.Y. Lin, Z. Zainal, N.E. Williams, K. Zhu, A.P. Kruzic, R.L. Smith, K. Rajeshwar, Bactericidal activity of TiO_2 photocatalyst in aqueous media: toward a solar-assisted water disinfection system, Environ. Sci. Technol. 28 (1994) 934–938.
[25] K. Wiench, W. Wohlleben, V. Hisgen, K. Radke, E. Salinas, S. Zok, R. Landsiedel, Acute and chronic effects of nano- and non-nano-scale TiO_2 and ZnO particles on mobility and reproduction of the freshwater invertebrate *Daphnia magna*, Chemosphere 76 (2009) 1356–1365.
[26] K. Hund-Rinke, M. Simon, Ecotoxic effect of photocatalytic active nanoparticles (TiO_2) on algae and daphnids, Environ. Sci. Pollut. Res. 13 (2006) 1–8.
[27] M. Heinlaan, A. Ivask, I. Blinov, H.C. Dubourguier, A. Kahru, Toxicity of nanosized and bulk ZnO, CuO and TiO_2 to bacteria *Vibrio fischeri* and crustaceans *Daphnia magna* and *Thamnocephalus platyurus*, Chemosphere 71 (2008) 1308–1316.
[28] M. Crisan, Ana Braileanu, M. Raileanu, D. Crisan1, V.S. Teodorescu, R. Birjega, V.E. Marinescu, J. Madarász, G. Pokol, TiO_2-based nanopowders obtained from different Ti-alkoxides, J. Therm. Anal. Calorim. 88 (2007) 171–176.
[29] International organization for standardization of water quality: determination of the inhibition of the mobility of *Daphnia magna* Straus (Cladocera, Crustacea). ISO 6341, 1996, Geneva, Switzerland.
[30] T. Lindgren, J.M. Mwabora, E. Avendano, J. Jonsson, A. Hoel, C.G. Granqvist, S.E. Lindquist, Photoelectrochemical and optical properties of nitrogen doped titanium dioxide films prepared by reactive DC magnetron sputtering, J. Phys. Chem. 107 (2003) 5709–5716.
[31] X. Wang, S. Meng, X. Zhang, H. Wang, W. Zhong, Q. Du, Multi-type carbon doping of TiO_2 photocatalyst, Chem. Phys. Lett. 444 (2007) 292–296.
[32] G. Kortü, Reflectance Spectroscopy, Springer Verlag, Berlin, 1969.
[33] C. Anderson, A.J. Bard, Improved photocatalytic activity and characterization of mixed TiO_2/SiO_2 and TiO_2/Al_2O_3 materials, J. Phys. Chem. B 101 (1997) 2611–2616.
[34] S. Jung, J.H. Kim, Sintering characteristics of TiO_2 nanoparticles by microwave processing, Korean J. Chem. Eng. 27 (2010) 645–650.
[35] H.M. Ali, M.M. Abou-Mesalam, M.M. El-Shorbagy, Structure and optical properties of chemically synthesized titanium oxide deposited by evaporation technique, J. Phys. Chem. Solids 71 (2010) 51–55.

[36] Associação Brasileira de Normas Técnicas (ABNT), Ecotoxicologia Aquática – Toxicidade aguda – Método de ensaio com *Daphnia* spp (Cladorera, Crustácea), ABNT NBR 12713 (2004).
[37] Organization for Economic Co-operation and Development (OECD), Paris, *Daphnia* 5P. Acute immobilization test. OECD Guideline for Testing of Chemicals, No. 202 (adapted 13.04.2004) (2004).
[38] K.N.P. Kumar, Growth of rutile crystallites during the initial-stage of anatase-to-rutile transformation in pure titania and in titania–alumina nanocomposites, Scr. Metall. Mater. 32 (1995) 873–877.
[39] W. Li, C. Ni, H. Lin, C.P. Huang, S.I. Shah, Size dependence of thermal stability of TiO_2 nanoparticles, J. Appl. Phys. 96 (2004) 6663–6668.
[40] T. Sasaki, M. Watanabe, Semiconductor nanosheet crystallites of quasi-TiO_2 and their optical properties, J. Phys. Chem. B 101 (1997) 10159–10161.
[41] O. Carp, C.L. Huisman, A. Reller, Photoinduced reactivity of titanium dioxide, Prog. Solid State Chem. 32 (2004) 33–177.
[42] I. Tunc, M. Bruns, H. Gliemann, M. Grunze, P. Koelsch, Bandgap determination and charge separation in Ag@TiO_2 core shell nanoparticle films, Surf. Interface Anal. 42 (2010) 835–841.
[43] R.I. Bickley, T. Gonzales-Carreno, J.L. Lees, L. Palmisano, R.J.D. Tilley, A structural investigation of titanium dioxide photocatalysts, J. Solid State Chem. 92 (1991) 178–190.
[44] Q. Zhang, L. Gao, J. Guo, Effects of calcination on the photocatalytic properties of nanosized TiO_2 powders prepared by $TiCl_4$ hydrolysis, Appl. Catal. B: Environ. 26 (2000) 207–215.
[45] T. Ohno, K. Sarukawa, K. Tokieda, M. Matsumura, Morphology of a TiO_2 photocatalyst (Degussa, P-25) consisting of anatase and rutile crystalline phases, J. Catal. 203 (2001) 82–86.
[46] G. Federici, B.J. Shaw, R.D. Handy, Toxicity of titanium dioxide nanoparticles to rainbow trout (*Oncorhynchus mykiss*): gill injury, oxidative stress, and other physiological effects, Aquat. Toxicol. 84 (2007) 415–430.
[47] D.B. Warheit, R.A. Hoke, C. Finlay, E.M. Donne, K.L. Reed, C.M. Sayes, Development of a base set of toxicity tests using ultrafine TiO_2 particles as a component of nanoparticle risk management, Toxicol. Lett. 171 (2007) 99–110.
[48] X. Zhu, Y. Chang, Y. Chen, Toxicity and bioaccumulation of TiO_2 nanoparticle aggregates in *Daphnia magna*, Chemosphere 78 (2010) 209–215.
[49] J.F. Reeves, S.J. Davies, N.J.F. Dodd, A.N. Jha, Hydroxyl radicals (•OH) are associated with titanium dioxide (TiO_2) nanoparticle-induced cytotoxicity and oxidative DNA damage in fish cells, Mutat. Res. 640 (2008) 113–122.
[50] S.B. Lovern, R. Klaper, *Daphnia magna* mortality when exposed to titanium dioxide and fullerene (C60) nanoparticles, Environ. Toxicol. Chem. 25 (2006) 1132–1137.
[51] S.H. Bang, T. L1, S.K. Lee, P. Kim, J.S. Kim, J. Min, Toxicity assessment of titanium (IV) oxide nanoparticles using *Daphnia magna* (water flea), Environ. Health Toxicol. 26 (2011) 1–6.
[52] A.G. Rincón, C. Pulgarín, Photocatalytical inactivation of *E. coli*: effect of (continuous-intermittent) light intensity and of (suspended-fixed) TiO_2 concentration, Appl. Catal. B 44 (2003) 263–284.
[53] J. Marugán, R. Grieken, C. Pablos, C. Sordo, Analogies and differences between photocatalytic oxidation of chemicals and photocatalytic inactivation of microorganisms, Water Res. 44 (2010) 789–796.
[54] N. Strigul, L. Vaccari, C. Galdun, M. Wazne, X. Liu, C. Christodoulatos, K. Jasinkiewicz, Acute toxicity of boron, titanium dioxide, and aluminum nanoparticles to *Daphnia magna* and *Vibrio fischeri*, Desalination 248 (2009) 771–782.
[55] K.T Kim, S.J. Klaine, J. Cho, S. Kim, S.D. Kim, Oxidative stress responses of *Daphnia magna* exposed to TiO_2 nanoparticles according to size fraction, Sci. Total Environ. 408 (2010) 2268–2272.